α-decay study of ^{218}Ac and ^{221}Th in ^{40}Ar+^{186}W reaction*

Wei Hua(滑伟)[1†] Zhiyuan Zhang(张志远)[2,3] Long Ma(马龙)[2] Zaiguo Gan(甘再国)[2,3]
Huabin Yang(杨华彬)[2] Minghui Huang(黄明辉)[2,3] Chunli Yang(杨春莉)[2,3]
Mingming Zhang(张明明)[2] Yulin Tian(田玉林)[2] Xiaohong Zhou(周小红)[2,3]
Cenxi Yuan(袁岑溪)[1] Caiwan Shen(沈彩万)[4] Long Zhu(祝龙)[1]

[1]Sino-French Institute of Nuclear Engineering and Technology, Sun Yat-sen University, Zhuhai 519082, China
[2]CAS Key Laboratory of High Precision Nuclear Spectroscopy, Institute of Modern Physics, Chinese Academy of Sciences, Lanzhou 730000, China
[3]School of Nuclear Science and Technology, University of Chinese Academy of Sciences, Beijing 100049, China
[4]School of Science, Huzhou University, Huzhou 313000, China

Abstract: In this study, ^{218}Ac and ^{221}Th nuclides were produced via the heavy-ion induced fusion evaporation reaction ^{40}Ar + ^{186}W. Their decay properties were studied with the help of the gas-filled recoil spectrometer SHANS and a digital data acquisition system. The cross section ratio between ^{222}Pa and ^{218}Ac was extracted experimentally, with measured value 0.69(9). Two new possible α decay branches to ^{221}Th are suggested. The valence neutron configurations for the daughter ^{217}Ra are discussed in terms of the hindrance factors.

Keywords: fusion-evaporation reaction, α decay, fine structure, reduced width, hindrance factor

DOI: 10.1088/1674-1137/abe0bd

I. INTRODUCTION

At the neutron-deficient side of the nuclear chart, the α decay is one of the dominating decay modes for heavy nuclides. In recent years, by utilising a gas-filled separator, many new nuclides in the A≈200 region close to the proton drip line were newly synthesized successfully via heavy-ion induced fusion-evaporation reactions [1-9]. The known α-decay characteristics of such nuclides and their descendants help to study the new properties in the decay chains. Among the evaporating channels, we cannot distinguish the 2p2n and 1α channels, which have the same evaporated residues (ERs). It is also known that, owing to the different decay energies, there might be differences between these two decay manners. Cross section is one of the probes in practice. In this mass region, a fine structure of the ground-state α decay is expected to be observed. However, owing to their low cross section, short survival time, and old technology, many of them have not been confirmed yet. In recent years, owing to the excellent separation performance of the gas-filled spectroscopy, fast data acquisition, and upgraded detector arrays, the uncleared α-decay fine structures could be elucidated.

In this paper, we will discuss the experimental results of ^{218}Ac and ^{221}Th in Section III. The details of the conducted experiments are presented in Section II.

II. EXPERIMENTAL METHODS

The experiments were performed at the Spectrometer for Heavy Atoms and Nuclear Structure (SHANS) [10] in Institute of Modern Physics (IMP), Lanzhou, China. A beam of ^{40}Ar with an energy of 198.7 MeV and an intensitiy of 300 pnA was provided by the Sector-Focusing Cyclotron (SFC) of the Heavy Ion Research Facility in Lanzhou (HIRFL). The ^{186}W target with average thickness of 200 μg/cm^2 was evaporated on a 50 μg/cm^2 of carbon, and covered with a 10 μg/cm^2 of carbon layer. The evaporated residues (ERs) yielded in the fusion-evaporation reaction ^{40}Ar + ^{186}W were filtrated by the separator SHANS and implanted into three 300- μm-thick position-sensitive strip detectors (PSSDs) with each active area of 50×50 mm^2. The front surface of each PSSD was divided into 16 strips along the perpendicular direction, leading to a horizontal position resolution of 3 mm. Eight additional non-position-sensitive side silicon detectors (SSDs) were mounted upstream, thereby forming a box geometry together with PSSDs. The total detection efficiency for the emitted α was measured to be ~72%. To distinguish the α events from the implanting events, two multi-wire proportional counters (MWPCs)

Received 26 November 2020; Accepted 5 January 2021; Published online 2 February 2021

* Supported by the National Natural Science Foundation of China (11805289, 11805291, 11875329), the Strategic Priority Research Program of Chinese Academy of Sciences (XDB34010000), and the National Key R&D Program of China (2018YFA0404402)

† E-mail: huaw@mail.sysu.edu.cn, corresponding author

were mounted 15 cm and 25 cm upstream from the PSSDs. Three extra non-position-sensitive silicon detectors, featuring the same size as the PSSDs, were installed side by side after the PSSDs to provide the veto signals from the light particles passing through the PSSDs. Near the charged particle detection system, two High Purity Germanium (HPGe) detectors and one clover detector were mounted at the right side, downward, and downstream, respectively. Signals from the preamplifiers of the Si-box, MWPCs, and veto detectors were recorded directly by a digital data acquisition system comprising sixteen V1724 waveform digitizers from CAEN S.p.A [11]. Every event was recorded in 30 μs -long trace at a sampling rate of 100 MHz. More details of the system could be found in Refs. [2,3,12]. Charged-particle energy calibration was performed using the ^{175}Lu target with the same beam. With the help of an alcohol circulation cooling system, the energy resolution for unpileup trace was approximately 40 keV (FWHM) for 6.5-10 MeV α particles, and the vertical position resolution was approximately 1.5 mm (FWHM). For pileup signals with $\triangle T > 1\mu$s, the typical energy resolution is 47 keV. However, for $\triangle T > 1\mu$s = 0.5-1 μs, the resolution worsens, becoming 70 keV. When the time difference is less than 100 ns, the extracted α energy from the pileup trace becomes unreliable.

When ERs trigger the PSSDs, the emitted α is called α_1. The ERs named as the mother nuclide decayed to the excited or ground states of the daughter nuclide, which might deexcite by α decay again, denoted as α_2. The same rule is applied to name α_3 for the α decay from the granddaughter nuclide following α_2. The aforementioned signals occurred at the same position in the PSSDs.

III. EXPERIMENTAL RESULTS

In the conducted experiment, some U, Pa, Th, and Ac isotopes were clearly identified, including ^{221}U, $^{220\text{-}222}$Pa, $^{219\text{-}222}$Th, ^{218,219}Ac, and ^{217,218}Ra. The 2D plotting of the correlated events is presented in Fig. 1; the time windows were 30 ms for ER- α_1 pairs and 50 ms for $\alpha_1 - \alpha_2$ pairs.

A. ^{218}Ac

When the time interval of α_1 and α_2 is in the order of a few hundred nanoseconds, the pluse piles upon the next one. Consequently, the two extracted energies will not be accurate anymore, but the sum energy value continues to be reliable; this was the case of ^{221}Pa, ^{219}Ac, and ^{220}Th clusters. Three waveforms of ^{221}Pa events are shown in Fig. 2 as examples. For this type of pairs, they distribute on an oblique line in the 2D plotting, such that the intercept is the sum of two energies. Similarly, the $E_{\alpha 1}$ energy peak projected from the ^{218}Ac events is broader than that of $E_{\alpha 2}$ from the ^{222}Pa ones. That is due to the short

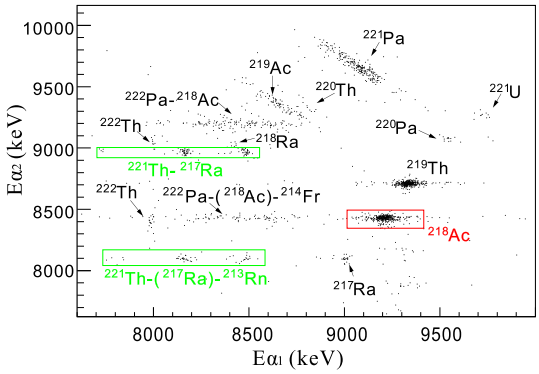

Fig. 1. (color online) Two-dimensional scatter plot of α-particle energies for correlated ER-$\alpha_1 - \alpha_2$ events measured in the PSSDs. The nuclide in parentheses indicate that the detection of their signals failed.

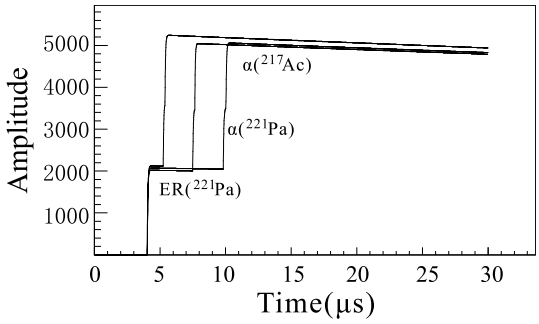

Fig. 2. Waveform examples of three ^{221}Pa-^{217}Ac events.

half-life of ^{218}Ac, whose energy could not be obtained accurately in the waveform.

Each cluster of events was checked carefully. Two components are observed in the time distribution of the ^{218}Ac events, shown in Fig. 3. The projected spectrum of these events displays a single-energy peak at 9205 keV, consistent with the previous measured values [13-15]. Thus, all of them are decaying from the ground state of ^{218}Ac. The isomer decay manner is not the right one, which could be excluded logically. The less-yields component (16%) is attributed to the indirect process, originated from the α decay of ^{222}Pa, whose emitted α particles failed to be detected. By solving the nonlinear nonhomogeneous first order differential equation with the approximation $\lambda_2 \gg \lambda_1$, the counts of ^{218}Ac $N(t)$ in the indirect process could be obtained.

$$\frac{\mathrm{d}N(t)}{\mathrm{d}t} = \lambda_1 N_0 e^{-\lambda_1 t} - \lambda_2 N(t) e^{-\lambda_2 t}. \quad (1)$$

Here, N_0 denotes the counts of ^{222}Pa that will decay to ^{218}Ac later. For each event, the ER trigger time was set to zero, so N_0 is independent of time; λ_1 and λ_2 are the decay constants of ^{222}Pa and ^{218}Ac, respectively.

Then, the second term shows the count ratio of α

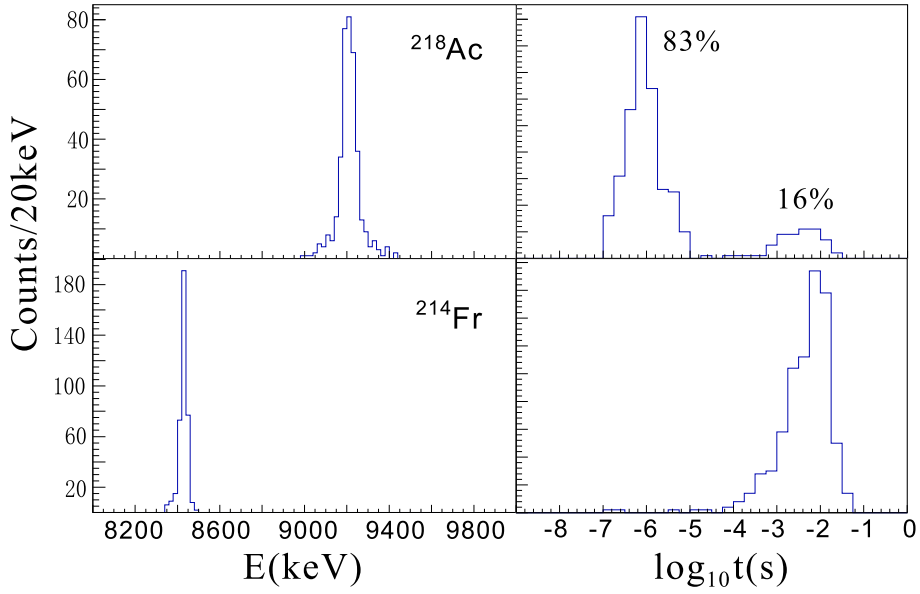

Fig. 3. (color online) The energy and time distribution of the events in the ^{218}Ac cluster, with ^{218}Ac in the upper part and ^{214}Fr in the lower part.

particles emitted from the ground state of ^{218}Ac, whose function corresponds to the time distribution curve. The maximum locates at $t=\frac{1}{\lambda_1}$, $10^{-2.33}$ here, whose value should correspond to the half life of ^{222}Pa. Directed by a 95.5% confidence level, a half-life of $3.24^{+1.13}_{-0.66}$ ms was obtained. This is consistent with the value $2.76^{+0.43}_{-0.33}$ ms deduced from the ^{222}Pa events(^{222}Pa-^{218}Ac and ^{222}Pa-(^{218}Ac)-^{214}Fr) in this study. The half-life of the another 83% component was derived to be $0.78^{+0.10}_{-0.08}$μs. They are the evaporation residues from the compound nuclide ^{226}U, i.e., the so called direct products. Thus, it refers to the ground state half-life of ^{218}Ac measured in this experiment.

When calculating the cross section of 1p3n channel (^{222}Pa) in this reaction, we should take into account the contribution from the indirect process, along with the direct one of the ^{222}Pa-^{218}Ac and the ^{222}Pa-(^{218}Ac)-^{214}Fr events. Simultaneously, the indirect part should be removed when counting the direct products ^{218}Ac. Given that the missing ratio when detecting the decaying α from ^{222}Pa and ^{218}Ac and their transporting efficiency provided by SHANS are almost same, the direct process ratio of $\frac{\sigma(^{226}\mathrm{U}^{*}\rightarrow 1p3n+^{222}\mathrm{Pa})}{\sigma(^{226}\mathrm{U}^{*}\rightarrow 3p5n+^{218}\mathrm{Ac})}$ deduced in this study is 0.69(9). The theoretical result computed by the Hivap2 code [16] with the commonly used parameters is 0.93. Further theoretical study by adjusting the fission barrier and the preformation factor is needed to analyze the experimental results.

B. ^{221}Th

The refine α-decay structure of ^{221}Th was investigated in many previous experiments [9,17-20]. However, only the branches with large ratios and the one that separates from the others clearly in energy scale were confirmed. In our measurements, besides the known α decays at 7731, 8164, and 8481 keV, two more small peaks were observed (shown in Fig. 4). The measured results in the present study and those in previous ones are compiled together in Table 1. For the sake of more accurate results, the listed energies and the half-lives of ^{217}Ra and ^{213}Rn were extracted from the ^{221}Th-^{217}Ra and ^{221}Th-(^{217}Ra)-^{213}Rn clusters, respectively, to achieve higher statistics. The ground state to ground state Q_α was deduced to be 8672(10) keV when corrected for the recoil energy and the screening effect of the atomic electrons. In Fig. 4, the α spectrum of ^{221}Th was obtained from the sum of ^{221}Th-^{217}Ra and ^{221}Th-(^{217}Ra)-^{213}Rn events. Meanwhile, the spectra of ^{217}Ra and ^{213}Rn were only extracted from the ^{221}Th-^{217}Ra cluster to clarify the correlation information. The statistical countings shown in the figure are 89 and 52 for ^{217}Ra and ^{213}Rn, respectively. Two peaks at 8409 and 8249 keV, highlighted in red, are the ones that were mentioned once as a short note in Ref. [17] without spectra shown. In this measurement, there were four 4-fold coincidence chains founded for these two branches, listed in Table 2. Chains 1-3 were the ones at 8409 keV, whereas chain 4 was located at 8249 keV. These multi-correlations help to partially (not sufficiently) support their existence in the fine decay structure. To demonstrate the existence of the two controversial branches, the γ spectrum correlated with the decaying α particles of the

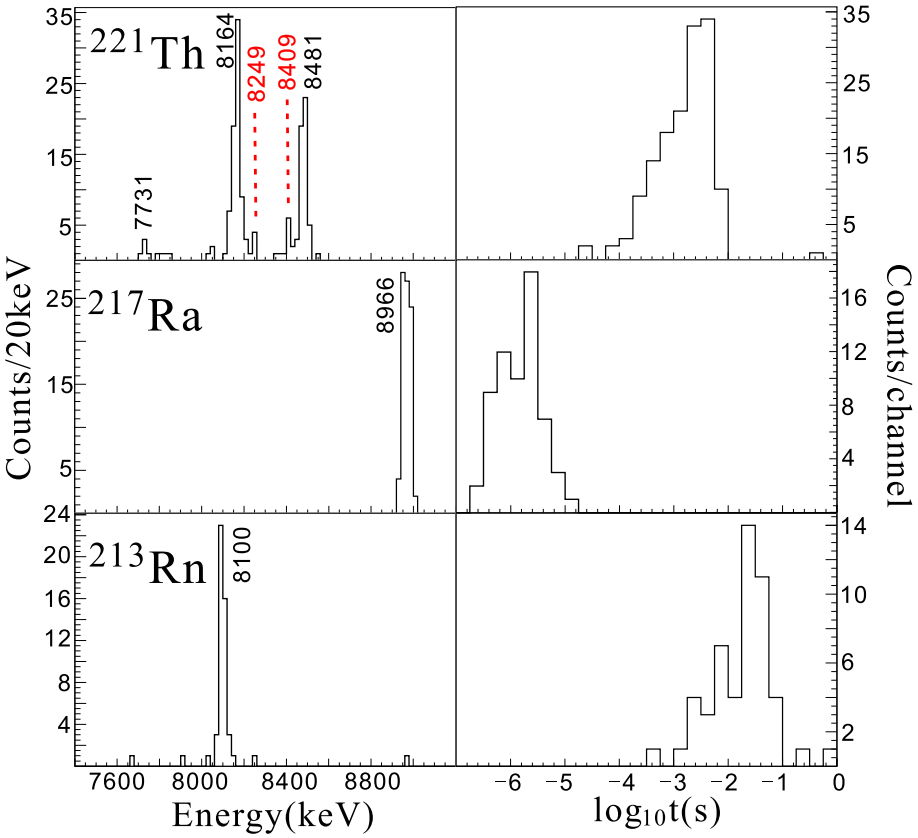

Fig. 4. (color online) Energy (left) and time distribution (right) of the events relative to the ^{221}Th decay chains. The previous indeterminate α branches are labeled in red.

Table 1. Measured results in this study compared with values previously reported in the literature.

Isotope	E_α/keV	Intensity(%)	$T^*_{1/2}$	Previous studies, E_α (Int.)	Previous studies, $T_{1/2}$
	7731(17)	3.5		7730(10) keV(6%)[17], 7733(8) keV(6.0%)[18], 7.73(1) MeV(8(3)%)[19], 7732(15) keV(4(3)%)[9]	
^{221}Th	8164(15)	52.5		8150(10) keV(53%)[17], 8146(5) keV(62.4%)[18], 8.145(10) MeV(62(5)%)[19], 8135(10) keV(48(9)%)[9], 8.11(4) MeV[20]	1.68(6) ms[18], 1.8(3) ms[19], $2.0^{+0.3}_{-0.2}$ ms[9], 1.0(2) ms[20]
	8249(19)	2.1	$1.95^{+0.38}_{-0.27}$ ms	8265(10)(4%)[17], 8.23(4) MeV[20]	
	8409(16)$^{\#}$	6.4$^{\#}$		8375(10) keV(11%)[17]	
	8481(15)	35.5		8470 keV(10%)[17], 8472(5) keV(31.6%)[18], 8.470(10) MeV(30(5)%)[19], 8458(10) keV(48(9)%)[9]	
^{217}Ra	8966(15)	100	$1.52^{+0.42}_{-0.27}$μs	8990(8) keV[18], 8.995(10) MeV[19], 8.99(4) MeV[20]	4(2)μs[9], 1.6(2)μs[19], 2.5(2)μs[20]
^{213}Rn	8100(15)		$15.88^{+5.47}_{-3.24}$ ms	8.085(10) MeV(99%)[19], 7.55(15) MeV(15)(1%)[19], 8.09(1) MeV[20], 7.98(1) MeV[20]	25.0(2) ms[19], 16(1) ms[20]

(*) 95.5% confidence level is used to compute the half-life error; (#) tentative assignment.

Table 2. Measured α-decay chains ER-$\alpha_1-\alpha_2-\alpha_3$ for the two dubious components. $E_{\rm ER}$, $E_{\alpha1}$, $E_{\alpha2}$, and $E_{\alpha3}$ are the energies of the evaporation residue, mother nuclide, daughter nuclide, and granddaughter nuclide, respectively; Δt is the decay time of the chain members.

Chain No.	$E_{\rm ER}$/keV	E_{α_1}/keV	Δt_{α_1}/ms	E_{α_2}/keV	Δt_{α_2}/μs	E_{α_3}/keV	Δt_{α_3}/ms
1	14059	8400	0.46	8958	3.00	8097	22.7
2	12498	8408	3.37	8968	3.18	8092	1.53
3	13462	8447	0.74	8971	1.98	8102	38.4
4	13100	8241	0.50	8953	0.68	8099	0.48

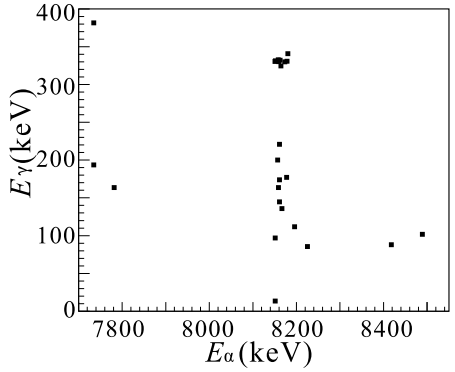

Fig. 5. $\alpha_1-\gamma$ plot.

Table 3. Reduced decay width and hindrance factor of ^{221}Th inferred from the experimental data. E_x and J^π are the energy and spin-parity of states in ^{217}Ra, respectively.

No.	E_α/keV	E_x/keV	J^π	l	δ^2/keV	HF
1	7731(17)	764(32)	$7/2^+$ [18]	0	40^{+8}_{-6}	$3.4^{+2.1}_{-0.5}$
2	8164(15)	323(30)	$11/2^+$ [24]	2	46^{+9}_{-6}	$2.9^{+1.8}_{-0.5}$
3	8249(19)	236(34)		2	$1.0^{+0.2}_{-0.1}$	134^{+82}_{-28}
4	8409(16)$^{\#}$	73(31)$^{\#}$		2	$1.1^{+0.2}_{-0.2}$	134^{+85}_{-17}
5	8481(15)	0	$9/2^+$ [24]	2	4^{+1}_{-1}	44^{+25}_{-3}

mother nuclei is presented as an additional argument (Fig. 5).

Only the γ peak at 331 keV could be recognized in the spectrum; it coincides with the emitted α at 8164 keV. This is consistent with previous γ information [21], i.e., γ decay from the excited state (323 keV, $11/2^+$) to the ground state $9/2^+$. The kinetic energy of the internal-conversion electrons from 331 keV γ will overlap on the 8164 keV α. With the known binding energy of electrons at K shell, i.e., 104 keV, an additional 227 keV energy will contribute to the counts at 8391 keV. Therefore, the small peak at 8409 keV may stem from the internal conversion effect. However, we cannot exclude the possible small branch decay to the level of 73 keV. This item is labeled with corner mark $^{\#}$ in Table 1 as a tentative result. Through the Band-Raman method, the internal conversion ratios were calculated to be 0.4 and 0.06 for $M1$ and $E2$ γ transitions, respectively. The upper-limit ratio deduced from this experiment was 0.12. Thus, this γ transition is mostly $E2$ type mixed with less $M1$. For the counts at 8249 keV, no other situations will generate them, except for a new decay branch. We list this item without the corner mark $^{\#}$.

The reduced α-decay width δ^2 [22] could be deduced from the experimental information, including decay energy, half-life, relative intensity, and angular momentum l taken away by the emitted α particles. In the case of odd-mass nuclide decay chain, the l value is related to the valence nucleus configuration of the parent and daughter nuclides. The hindrance factor (HF) of the odd-mass nuclide is the factor normalized to δ^2_{ee} (the ground state transition of the neighboring even-even nuclide). It could help us to elucidate the centrifugal barrier effect and discuss the configuration assignments.

It is well known that even-even nuclides are unhindered in general. The value of ^{222}Th is 134^{+109}_{-41}, according to this experiment. We used this value as δ^2_{ee} to calculate the hindrance factors of ^{221}Th, for which the $\Omega = 1/2$, $i_{11/2}$ neutron orbital dominates the ground state $7/2^+$[23]. The α-decay widths calculated from the present data are tabulated in Table 3; l was set to be 0, 2, and 2 for branches 1, 2, and 5, respectively, according to the previous spin-parity assignments [3] and the conservation law of parity and angular momentum. By employing the data listed in Table 1 and the aforementioned l, the g.s to g.s decay shows an HF of 44, while decays from g.s to the excited states at 764(23) and 323(20) keV are much less retarded with HF 3. The nuclei investigated here are expected to be dominated by the shell model orbital $g_{9/2}$, while $i_{11/2}$ and $j_{15/2}$ also have certain contributions. In shell model calculation, the states dominated by $\nu j_{15/2}$ lie higher than others. Thus, the possibility of $\nu j_{15/2}$ is excluded at the first step. In the in-beam γ spectra study of ^{217}Ra [24], the ground state was assigned to $9/2^+$ with the configuration of $\nu g^3_{9/2}$(seniority number = 1). Concerning the ground state of ^{221}Th, the odd neutron is regarded to mainly occupy the $i_{11/2}$ orbital at moderate axial quadrupole-octupole deformation [25]. These terms strongly hinder the α decay from the ground state $7/2^+$(^{221}Th) to the ground state $9/2^+$(^{217}Ra). Both $\nu g^3_{9/2}$ and $\nu g^2_{9/2} i_{11/2}$ could give rise to the $11/2^+$ state at 323 keV, but its small HF value proposes its final valence neutron occupation to be the same as that of the ground state of ^{221}Th, that is, $\nu i_{11/2}$. Regarding the level at 764 keV, the HF value is as small as that of the $11/2^+$ state, no matter taking either l=0 or 2. Consequently, it has the same configuration, $\nu g^2_{9/2} i_{11/2}$, and keeps the earlier assignment $7/2^+$. Similar to the $9/2^+$ state, the levels at 73 and 236 keV (identified from 8249- and 8409-keV α) have larger HF values increased by two orders of magnitude, regardless of the value of l assigned. Thus, the configuration $\nu g^3_{9/2}$ is expected for those two states tentatively. Further γ spectra studies on these levels are required to specify the J^π assignments.

IV. CONCLUSION

In this study, several U, Pa, Th, and Ac isotopes (^{221}U, $^{222\text{-}220}$Pa, $^{219\text{-}222}$Th, ^{218,219}Ac, ^{217,218}Ra) were produced via the fusion-evaporation reaction ^{40}Ar (^{186}W, $xpxn$) in the Institute of Modern Physics, Chinese Academy of Sciences. They were separated by SHANS and identified by the charged-particle and γ detector array at the terminal.

Some products of ^{218}Ac came from the direct process (ERs of the compound nuclide ^{226}U), specifically those left from the indirect process (α decay from the mother nuclide ^{222}Pa). After excluding the indirect yields, the cross section ratio between ^{222}Pa and ^{218}Ac is 0.69(9), while the HIVAP2 calculation result is 0.93. By checking the multi-correlation and correlated γ spectrum, the refine α decay structure of ^{221}Th was analyzed in this study. We suggest the existence of the branch with decay α at 8249 keV but could not exclude the existence of the one decayed via 8409 keV α. Their large hindrance factors indicate the $g_{9/2}$ occupation of the valence neutron at those two excited states in ^{217}Ra. The $\nu g^3_{9/2}$ configuration is suggested for them in this study. In future studies, further γ spectra information is needed to provide supplementary evidence.

ACKNOWLEDGEMENTS

The authors would like to thank the colleagues of the SHANS and accelerator groups at the Institute of Modern Physics, Chinese Academy of Sciences, who provided great support for the experiment.

References

[1] J. Khuyagbaatar, A. Yakushev, Ch. E. Düllmann *et al.*, Phys. Rev. Lett. **115**, 242502 (2015)
[2] Z. Y. Zhang, Z. G. Gan, H. B. Yang *et al.*, Phys. Rev. Lett. **122**, 192503 (2019)
[3] L. Ma, Z. Y. Zhang, Z. G. Gan *et al.*, Phys. Rev. Lett. **125**, 032502 (2020)
[4] M. D. Sun, Z. Liu, T.H. Huang *et al.*, Phys. Lett. B **771**, 303 (2017)
[5] H. B. Yang, L. Ma, Z. Y. Zhang *et al.*, Phys. Lett. B **777**, 212 (2018)
[6] H. B. Yang, Z. Y. Zhang, J. G. Wang *et al.*, Eur. Phys. J. A **51**, 88 (2015)
[7] T. H. Huang, W. Q. Zhang, M. D. Sun *et al.*, Phys. Rev. C **96**, 014324 (2017)
[8] T. H. Huang, W. Q. Zhang, M. D. Sun *et al.*, Phys. Rev. C **98**, 044302 (2018)
[9] F. P. Heβberger, S. Hofmann1, D. Ackermann *et al.*, Eur. Phys. J. A **8**, 521 (2000)
[10] Z. Y. Zhang, L. Ma, Z. G. Gan *et al.*, Nucl. Instrum. Method Phys. Res., Sect. B **317**, 315 (2013)
[11] V1724 and VX1724 User Manual, 2018, http://www.caen.it/csite
[12] H. B. Yang, Z. G. Gan, Z. Y. Zhang *et al.*, Eur. Phys. J. A **55**, 8 (2019)
[13] J. Borggreen, K. Valli, and E. K. Hyde, Phys. Rev. C **2**, 1841 (1970)
[14] N. Schulz, A. Chevallier, J. Chevallier *et al.*, Phys. Rev. C **28**, 435 (1983)
[15] H. Miyatake, K. Sueki, H. Kudo *et al.*, Nucl. Phys. A **501**, 557 (1989)
[16] W. Reisdorf, Z. Phys. A, **300**: 227 (1981)
[17] A. N. Andreyev, D. D. Bogdanov, V. I. Chepigin *et al.*, Z. Phys. A **337**, 229 (1990)
[18] NNDC National Nuclear Data Center, Chart of Nuclides, https://www.nndc.bnl.gov/nudat2
[19] D. F. Torgenson and R. D. Macfarlane *et al.*, Nucl. Phys. A **149**, 641 (1970)
[20] K. Valli, E. K. Hyde, J. Borggreen *et al.*, Phys. Rev. C **1**, 2115 (1970)
[21] A. K. Mistry, J. Khuyagbaatar, F.P. Heβberger *et al.*, Nucl. Phys. A **987**, 337 (2019)
[22] J. O. Rasmussen, Phys. Rev. **115**, 1675 (1959)
[23] G. A. Leander and Y. S. Chen, Phys. Rev. C **37**, 2744 (1988)
[24] N. Roy, D. J. Decman, H. Kluge *et al.*, Nucl. Phys. A **426**, 379 (1984)
[25] W. Reviol, D. G. Sarantites, C. J. Chiara *et al.*, Phys. Rev. C **80**, 011304 (2009)